1096.
(6) Maruca, R.; Schaeffer, R. *Inorg. Chem.* **1970**, *9*, 2161.
(7) Hall, L. H.; Koski, W. S. *J. Am. Chem. Soc.* **1962**, *84*, 4205.
(8) Boocock, S. K.; Greenwood, N. N.; Kennedy, J. P.; Taylorson, D. *J. Chem. Soc., Chem. Commun.* **1979**, 16. Greenwood, N. N.; Kennedy, J. D.; McDonald, W. S.; Staves, J.; Taylorson, D. *Ibid.* **1979**, 17.
(9) Greenwood, N. N.; Kennedy, J. D.; Spalding, T. R.; Taylorson, D. *J. Chem. Soc., Dalton Trans.* **1979**, 840.
(10) Brown, G. M.; Pinson, J. W.; Ingram Jr., L. L. *Inorg. Chem.* **1979**, *18*, 1951.
(11) DuPont, J. A.; Hawthorne, M. F. *J. Am. Chem. Soc.* **1964**, *86*, 1643.
(12) Hawthorne, M. F.; Owen, D. A. *J. Am. Chem. Soc.* **1968**, *90*, 5912.
(13) Burg, A. B.; Reilly, T. J. *Inorg. Chem.* **1972**, *11*, 1962.
(14) Plotkin, J. S.; Sneddon, L. G. *J. Chem. Soc., Chem. Commun.* **1976**, 95.
(15) Pretzer, W. R.; Rudolph, R. W. *Inorg. Chem.* **1976**, *15*, 1779.
(16) Dobbie, R. C.; Distefano, E. W.; Black, M.; Leach, J. B.; Onak, T. *J. Organomet. Chem.* **1976**, *114*, 233.
(17) Plotkin, J. S.; Astheimer, R. J.; Sneddon, L. G. *J. Am. Chem. Soc.* **1979**, *101*, 4155.
(18) Hosmane, N. S.; Grimes, R. N. *Inorg. Chem.* **1979**, *18*, 2886.
(19) Ulman, J. A.; Fehlner, T. P. *J. Am. Chem. Soc.* **1976**, *98*, 1119.
(20) Beltram, G. A.; Fehlner, T. P. *J. Am. Chem. Soc.* **1979**, *101*, 6237.
(21) Fehlner, T. P. *Inorg. Chem.* **1975**, *14*, 934.
(22) Shriver, D. F. "The Manipulation of Air-Sensitive Compounds"; McGraw-Hill: New York, 1969.
(23) Klein, M. J.; Harrison, B. C.; Solomon, I. J. *J. Am. Chem. Soc.* **1958**, *80*, 4149.
(24) First reported by Burg and Reilly, ref 13.
(25) An uncharacterized white solid was also observed by Burg and Reilly, ref 13.
(26) The reaction of 1,5-$C_2B_3H_5$ with $Fe(CO)_5$ yields $C_2B_3H_5Fe(CO)_3$ among other products: Miller, V. R.; Sneddon, L. G.; Beer, D. C.; Grimes, R. N. *J. Am. Chem. Soc.* **1974**, *96*, 3090.
(27) Dewar, J. S.; Thiel, W. *J. Am. Chem. Soc.* **1977**, *99*, 4899. Thiel, W. *QCPE* **1978**, *11*, 353.
(28) Dewar, M. J. S.; McKee, M. L. *J. Am. Chem. Soc.* **1977**, *99*, 5231.
(29) Guest, M. F.; Hillier, I. H. *Mol. Phys.* **1973**, *26*, 435.
(30) Dixon, D. A.; Kleier, D. A.; Halgren, T. A.; Hall, J. H.; Lipscomb, W. N. *J. Am. Chem. Soc.* **1977**, *99*, 6226.
(31) Ulman, J. A.; Fehlner, T. P. *J. Am. Chem. Soc.* **1978**, *100*, 449.
(32) Rabalais, J. W. "Principles of Ultraviolet Photoelectron Spectroscopy"; Wiley-Interscience: New York, 1977.
(33) Dewar, M. J. S.; McKee, M. L. *Inorg. Chem.* **1978**, *17*, 1569.
(34) Onak, T.; Wan, E. *J. Chem. Soc., Dalton Trans.* **1974**, 665.
(35) Wilson, E. B., Jr.; Decius, J. C.; Cross, P. C. "Molecular Vibrations"; McGraw-Hill: New York, 1955.
(36) Jotham, R. W.; Reynolds, D. J. *J. Chem. Soc. A* **1971**, 3181.
(37) σ and π refer to the symmetry of the orbital with respect to the radial direction of an exopolyhedral bond. This designation can be ambiguous. For example, in $B_6H_6^{2-}$, the t_{2g} orbitals interact with exopolyhedral ligands in a π fashion only while the t_{1u} orbitals can interact in both σ and π fashions. It is found in terms of PES (ref 20) that the t_{1u} π interaction is relatively small; hence only the t_{2g} orbitals were considered as π orbitals. As the latter are constructed mainly of p functions that are tangential to the surface of the sphere that holds the cage atoms, we also refer to these orbitals as surface orbitals.
(38) Note that, as one-half of the D_{2h} dimer is twisted, the bonding and antibonding components will become degenerate.
(39) As the symmetry becomes lower this type of assignment becomes more arbitrary and less meaningful, especially in terms of the exo σ and endo σ designations.
(40) See Figure 6 for the axes used.
(41) The HOMO shows little variation in the x–x bond order, but the totals in Table VI show this interaction to be important.
(42) McNeill, E. A.; Gallaher, K. L.; Scholer, F. R.; Bauer, S. H. *Inorg. Chem.* **1973**, *12*, 2108.

Electron Spin–Echo Studies of Radical Interaction and Orientation on Catalytic Surfaces. CH_2OH Radicals in A-, Y-, and X-Type Zeolites

Tsuneki Ichikawa and Larry Kevan*

Contribution from the Department of Chemistry, Wayne State University, Detroit, Michigan 48202. *Received October 10, 1979*

Abstract: CH_2OH radicals have been generated by γ-radiolysis at 77 K from methanol adsorbed on Na-A, Na-Y, Na-X, and K-X type zeolites. The electron spin resonance spectra of the radicals on the different zeolites are similar. However, electron spin-echo modulation patterns associated with aluminum nuclei in the zeolites are observed at 4 K and show differences between the different zeolites. These spin-echo results have been simulated in order to obtain structural information about the adsorbed radical site. Each radical interacts with one Si or Al nucleus at 3.4 Å in Na^+-containing zeolites and at 3.6 Å in K^+-containing zeolites. From these data and from structural data on the zeolites the CH_2OH radical is suggested to be located in an α cage with its molecular dipole oriented toward a cation in the center of the square (X and Y zeolite) or hexagonal (A zeolite) faces of the α cage. The COH plane is aligned along a diagonal of the square face so that the radical site is oriented toward one Al or Si nucleus. The utility of electron spin-echo modulation analysis to probe the orientation of adsorbed species relative to the surface is emphasized.

Introduction

The characterization of the structure of reactive intermediates adsorbed on surfaces is of major importance for elucidation of the chemical pathways in heterogeneous catalysis. For paramagnetic intermediates electron spin resonance (ESR) is a primary method of characterization. Extensive work has been carried out in this area,[1] the general focus of which has been to measure deviations of radical hyperfine parameters for radicals adsorbed on surfaces compared to radicals trapped in bulk solids. These changes in hyperfine parameters have typically been interpreted in terms of a change in the radical structure itself or in its electron distribution due to strong surface electric fields. Although interesting and significant, such studies have not generally led to information about the orientation and interaction distances of the radicals *relative to the surface atoms*. Such information is potentially contained in hyperfine interactions which are usually too weak to be seen in normal ESR experiments.

In the last several years we have shown that the weak hyperfine interactions characterizing the average surroundings of a trapped radical in a *disordered matrix* can often be quantitatively analyzed from electron spin-echo modulation patterns.[2-4] In particular, the *detailed* solvation geometry of solvated electrons[2,3,5-8] and of selected anions,[9] atoms,[10-12] and cations[13] in frozen solutions has been elucidated for the first time. In general, one can identify the type, number, distance, and isotropic hyperfine coupling of magnetic nuclei within about 2-6 Å from the unpaired electron on a radical.[14]

Here, we show how electron spin-echo modulation analysis can be applied to study the local environment of radicals ad-

0002-7863/80/1502-2650$01.00/0

sorbed on surfaces. Specifically, we present new information on the location and orientation of the CH_2OH radical on the interior cage surfaces of X-, Y-, and A-type zeolites, which are hydrated aluminosilicates widely used as heterogeneous catalysts.[15] By using zeolites of different structural types we are able to relate the zeolite structure to the CH_2OH radical location and reach more detailed structural conclusions than were possible in a recent study of the CH_2OH radical in only A-type zeolites.[16]

Experimental Section

Zeolites 3A (K-A), 4A (Na-A), 13X (Na-X), and 30-200Y (Na-Y) were obtained as powders from Linde Co. The symbols in parentheses indicate the cation and the structural type of zeolite. K-X and K-Y zeolites were made from the sodium zeolites by ion exchange in a stirred slurry of 1 M KCl at 100 °C, washing with distilled water to remove chloride, and drying at 80 °C for 24 h. Nearly complete exchange is achieved by repeating this procedure three times. The zeolite samples were dehydrated in 3-mm o.d. Suprasil quartz tubes at 150 °C for ~4 h and then at 350 °C for ~10 h under a vacuum of $\sim 1 \times 10^{-2}$ Pa. Methanol was adsorbed at room temperature by exposing the saturation vapor pressure of methanol to the zeolite for ~2 h. The samples were then sealed off and γ-irradiated with ^{60}Co to a dose of 0.1 Mrad at 77 K in the dark.

ESR spectra were obtained on a Varian E-4 spectrometer. Electron spin-echo signals were obtained on a home-built spectrometer that has been described.[10,12] The microwave pulse width was 100 ns so that proton modulation was suppressed and only aluminum modulation was observable. Typical pulse powers were 20 W and all experiments were carried out at 4.2 K.

Theory and Data Analysis

The theory and applications of electron spin-echo modulation have been described in detail[14] so only the final formulas used to calculate the modulation are given. The normalized two-pulse echo modulation as a function of τ, the time between the pulses, for the case of weak hyperfine interaction ($r > \sim 3$ Å) and negligible quadrupole interaction is given by

$$V(\tau) = [1 - (1 - \cos \omega_\alpha \tau)(1 - \cos \omega_\beta \tau)(k'/2)] \quad (1)$$

where

$$k' = (\omega_I B/\omega_\alpha \omega_\beta)^2 (4/3) I(I+1)$$

$$\omega_\alpha = [(\tfrac{1}{2}A + \omega_I)^2 + (\tfrac{1}{2}B)^2]^{1/2}$$

$$\omega_\beta = [(\tfrac{1}{2}A - \omega_I)^2 + (\tfrac{1}{2}B)^2]^{1/2}$$

$$A = \frac{g g_n \beta \beta_n}{\hbar r^3}(3\cos^2\theta - 1) - 2\pi a$$

$$B = \frac{3 g g_n \beta \beta_n}{\hbar r^3} \sin\theta \cos\theta$$

In the above expressions ω_I is the nuclear Larmor frequency in the field H_0, ω_α and ω_β are the hyperfine frequencies associated with the electron spin levels $|\tfrac{1}{2}\rangle$ and $|-\tfrac{1}{2}\rangle$, a is the isotropic hyperfine coupling constant, r is the electron-nuclear distance and θ is the angle between H_0 and the r vector. For a disordered system the total modulation is obtained by averaging over all the orientations θ. Further, if the electron interacts with n identical nuclei, the overall modulation is given by

$$V_{mod} = [\langle V(r,a) \rangle]^n \quad (2)$$

where the angular brackets indicate the averaging over all the orientations. It is this expression which was programmed numerically to calculate the modulation.

The experimental data were analyzed using the ratio analysis method described by Ichikawa et al.[7] First, two smooth curves joining all the maxima and all the minima of the echo modulation are drawn. These curves are denoted by V_{max}^{ex} and V_{min}^{ex}, respectively. Experimentally the ratio $R^{ex} = V_{max}^{ex}/V_{min}^{ex}$ is determined for the same value of τ as a function of τ. The advantage of this method is that $R^{ex}(\tau)$ is independent of the echo decay function. This is compared with the theoretical ratio

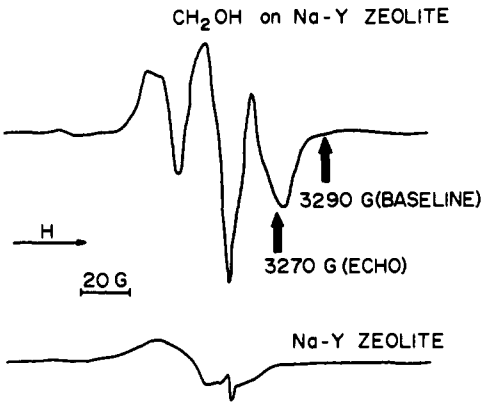

Figure 1. ESR spectra of γ-irradiated Na-Y zeolite (lower) and of CH_2OH on γ-irradiated Na-Y zeolite (upper) at 77 K. The radiation dose was 0.2 Mrad. The arrows show the magnetic field at which electron spin-echoes and their associated base line were measured.

$$R^{th}(\tau) = \left[\frac{V_{max}^{th}(\tau)}{V_{min}^{th}(\tau)}\right]^n = (r^{th})^n \quad (3)$$

where the theoretical maxima and minima are given when $\cos \omega_{\alpha,\beta}\tau = \pm 1$. For a system with n equivalent nuclei

$$R^{th} \simeq [r^{th}(a,r)]^n$$

$$\log\log R^{th} = \log n + \log\log r^{th} \quad (4)$$

Thus, a convenient way of analyzing the modulation curves is to plot $\log\log R^{ex}$ and $\log\log r^{th}$ vs. τ. Such a plot gives two parallel curves displaced along the y axis by $\log n$ provided that correct values for r and a are chosen. Thus, a and r are varied till nearly parallel curves are obtained. The shift needed to bring these curves into coincidence gives $\log n$ and hence n. The parameters obtained from the ratio analysis are used to simulate the modulation. In order to compare the calculated modulation with the experimental curve, the normalized modulation is multiplied with a generalized decay function $g(\tau)$ of the form

$$g(\tau) = \exp(A_0 + A_1\tau + A_2\tau^2 + A_3\tau^3) \quad (5)$$

The coefficients A_i are determined by a least-squares method.[7]

This analysis will be applied to ^{27}Al modulation for which $I = \tfrac{5}{2}$. Although the quadrupole moment of ^{27}Al is relatively large, we neglect the quadrupole interaction on the modulation pattern because it is too complicated to include rigorously.[18] Quadrupole interaction may be approximately included in the modulation analysis if the quadrupole corrections to the energy levels are less than the electron dipolar corrections. The effect of a small quadrupole correction on the modulation pattern is similar to that of a small isotropic hyperfine coupling.[14,20] In the simulations we found good fits to the experimental data for zero isotropic coupling; this seems to justify neglect of the quadrupole interaction for ^{27}Al in these systems.

Results

ESR spectra of γ-irradiated Na-Y zeolite without and with adsorbed methanol are shown in Figure 1. Spectra of the other zeolites were similar. With adsorbed methanol the well-known[17] triplet spectrum of CH_2OH is observed. It can be seen that the background ESR spectrum in the zeolite without adsorbate overlaps the low-field portion of the CH_2OH spectrum but that there is little interference with the high-field line of CH_2OH. Spin-echo signals were therefore obtained by mon-

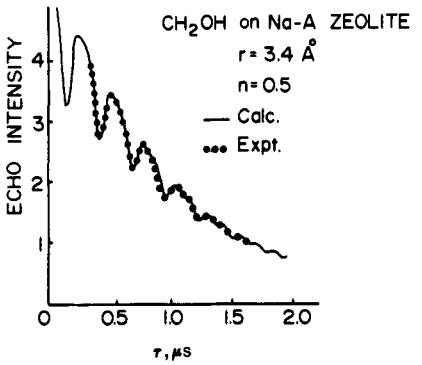

Figure 2. Comparison of the experimental (···) and calculated (—) two-pulse electron spin-echo aluminum modulation for CH_2OH on Na-A zeolite. The decay function used is $\exp(1.67 - 0.67\tau - 0.40\tau^2 - 0.13\tau^3)$.

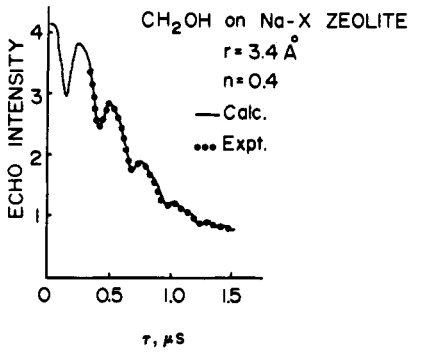

Figure 3. Comparison of the experimental (···) and calculated (—) two-pulse electron spin-echo aluminum modulation for CH_2OH on Na-X zeolite. The decay function used is $\exp(1.42 + 0.22\tau - 2.39\tau^2 - 1.03\tau^3)$.

itoring the high-field line at 3270 G as shown in Figure 1. The spin-echo base line was obtained by moving the field off resonance to 3290 G as also shown.

Two pulse electron spin-echo signals were recorded vs. τ, the time between the two pulses. The echo decay is modulated with a frequency close to the free nuclear frequency of ^{27}Al, which is 3.6 MHz in a 3270-G field. The same modulation frequency was observed in both Na and K zeolites, indicating that the observed modulation is due to Al nuclei in the zeolite lattice. Modulation due to ^{23}Na, ^{39}K, and ^{1}H would occur at 3.7, 0.65, and 13.9 MHz, respectively. Sufficiently long microwave pulses (100 ns) were used so that ^{1}H modulation does not appear. The 1.5-μs modulation period of ^{39}K is similar to the decay time of the electron spin-echo signal and so is difficult to observe. The ^{23}Na modulation frequency is close to that of ^{27}Al and could contribute to the observed modulation. However, previous studies on Ca-A zeolite have shown that all the observed modulation can be attributed to ^{27}Al nuclei.[16]

Figures 2-5 show the experimental and simulated modulation patterns for Na-A, Na-X, K-X, and Na-Y zeolites, respectively. The data were analyzed using the ratio analysis described above. The best fit values of n and r are given in the figures and the decay constants are given in the figure captions. In each case the best fit value of the isotropic hyperfine coupling was zero.

In K-A zeolite no CH_2OH radicals were formed. This is because methanol is presumably too large to enter the α cage of this zeolite. In K-Y zeolite the electron spin-echo signal decayed in less than 1 μs and the modulation depth was too shallow for a quantitative analysis.

Discussion

Our analysis shows that each CH_2OH radical interacts with an average of less than one Al nucleus in the zeolite lattice. At

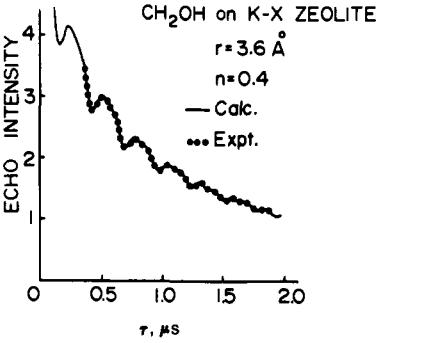

Figure 4. Comparison of the experimental (···) and calculated (—) two-pulse electron spin-echo aluminum modulation for CH_2OH on K-X zeolite. The decay function used is $\exp(1.76 - 1.60\tau - 0.65\tau^2 - 0.14\tau^3)$.

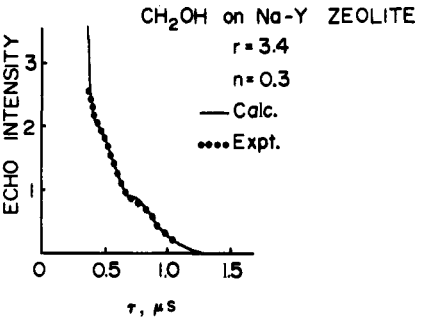

Figure 5. Comparison of the experimental (···) and calculated (—) two-pulse electron spin-echo aluminum modulation for CH_2OH on Na-Y zeolite. The decay function used is $\exp(6.16 - 21.8\tau - 28.2\tau^2 - 13.8\tau^3)$.

Table I. Average Number of Al Atoms in Various Zeolites Interacting with Adsorbed CH_2OH Radicals

zeolite	av no. of interacting Al nuclei	Al/(Al + Si) mole ratio
Na-A	0.5	0.50
Na-X	0.4	0.45
K-X	0.4	
Na-Y	0.3	0.30

Table II. Al-CH_2OH Radical Distances in Zeolites

zeolite	Al-CH_2OH distance, Å	zeolite	Al-CH_2OH distance, Å
Na-A	3.4 ± 0.5	Na-X	3.4
Na-Y	3.4	K-X	3.6

first glance this appears rather nonphysical. However, an explanation is provided in Table I. The average number of interacting aluminum nuclei is seen to correlate with the Al to (Al + Si) mole ratio in the A, X, and Y zeolite structures. The zeolite lattice is composed of silica and alumina tetrahedra so that silicon and aluminum atoms occupy equivalent positions with respect to a radical within the lattice. It thus appears that each CH_2OH radical interacts with an average of *one* aluminum or silicon nucleus. Since only the aluminum nuclei are magnetic the average number of observed (i.e., Al) nuclei varies as the Al to (Al + Si) mole ratio. One implication of this conclusion is that the Al-CH_2OH interaction distance should not depend on the Al mole ratio in structurally different zeolites.

Table II shows the Al to CH_2OH radical distances in the different zeolites. For Na-X, Na-Y, and Na-A zeolites the distance is constant at 3.4 Å. This constancy is consistent with the above data in showing that each radical interacts with only one Al or Si nucleus. The second interesting point is that the

Al-CH_2OH distance seems significantly larger for K-X zeolite compared to Na-X zeolite. Although the K-Y zeolite data could not be analyzed quantitatively, it does show less deep modulation than the Na-Y zeolite, which is consistent with a larger interaction distance in the K-Y zeolite.

The ionic radii of Na^+ and K^+ are 0.95 and 1.33 Å, respectively.[21] Thus, the 0.2 Å greater Al-CH_2OH distance in K-X zeolite implies that the location of the CH_2OH radical in the zeolite cage is dependent on the cation charge-methanol dipole interaction. The larger diameter cation causes the CH_2OH radical to move further into the zeolite cage since the cations are thought to reside on or slightly below the interior cage surfaces. This increases the Al-CH_2OH distance as observed.

Before discussing a specific picture of the CH_2OH radical location in zeolite cages we must describe the zeolite structure in more detail.[15] Zeolites are composed of interconnected AlO_4 and SiO_4 tetrahedra. The structure is most easily discussed in terms of polyhedra formed by interconnecting the Al and Si atoms; the Si-Al distance is 3.1 Å. For the A, X, and Y zeolites the building block is a cuboctahedron having eight hexagonal and six square faces which is called the sodalite unit or β cage. In A-type zeolite the sodalite units are interconnected by cubes on some of their square faces to form a supercage or α cage composed of 12 square, 8 hexagonal, and 6 octagonal faces. The octagonal face provides the largest opening with a 4.2-Å diameter. In X- and Y-type zeolites the sodalite units are interconnected by hexagonal prisms on some of their hexagonal faces to form an α cage composed of 18 square, 4 hexagonal, and 4 dodecagonal faces.

There is some uncertainty about the location of the cations in dehydrated zeolites but a recent review[15] gives the following. In Na-A zeolite eight Na^+ are near the centers of the hexagonal faces of the α cage and four Na^+ are offset from the center of the octagonal faces of the α cage. In Na-X, Na-Y, K-X, and K-Y zeolites about 30 cations are displaced from the center of the hexagonal prisms into the sodalite cages (site I′) and another ~30 cations are displaced into the sodalite cages from the centers of the square faces bordering the α cage (site II′). The cations in site II′ are best located for interaction with adsorbed molecules in the α cage.

Methanol has a molecular radius of ~1.6 Å, which is too large to enter the β cage (2.2-Å entrance diameter), so the adsorbed methanol molecules will be in the α cage. A suggested geometry for the adsorbed CH_2OH radical is shown in Figure 6. One square face of the α cage in either A-, X-, or Y-type zeolite is shown; in A-type zeolite this can also be a hexagonal face since cations are located in these faces. The cation is located below the center of this face in the β cage by an arbitrary 1 Å in this figure. The molecular dipole of methanol approximately bisects the COH angle[22] and is shown oriented toward the cation; this orientation is suggested by the cation effect on the radical-aluminum distance as discussed above. The COH plane in the radical is rotated to place it along a diagonal of the square face so that the radical site (i.e., the CH_2 group) is in the direction of an aluminum at one corner of the face. Thus, the radical interacts with only one Al nucleus as found experimentally. For an Al to radical distance of 3.4 Å the oxygen in the radical is 2.5 Å above the α-cage face. In this geometry the distance between the radical site and Na^+ is 4.5 Å. At this distance Na^+ modulation would be negligible compared to Al modulation at 3.4 Å.

In a previous study of CH_2OH in Na-A zeolite it was assumed that the radical site does not interact with any specific Al nucleus and the modulation depth was simulated by a lattice sum over all nuclei in the α cage.[16] This analysis led to the conclusion that the radical was located 2-3 Å from the center of the α cage and no preferred orientation was suggested. With our additional data involving the larger cages in the X and Y zeolites we find the same radical-aluminum interaction distance for A, X, and Y zeolites so it seems that the radical is located nearer to the cage surface than to the center of the cage and interacts most strongly with only one Al nucleus. Thus, the more detailed model of Figure 6 can be suggested.

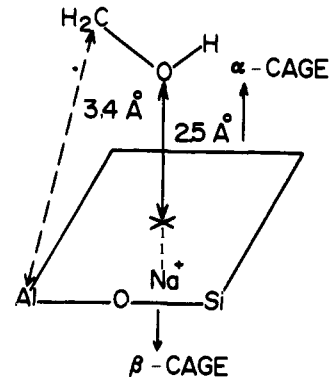

Figure 6. Suggested geometry for an adsorbed CH_2OH radical in a zeolite cage. A square face of the α cage in A-, X-, or Y-type zeolites having Al or Si at each corner is shown. The cation is located below the center of this face in the β cage. In A-type zeolite this can also be a hexagonal face since cations are located in these faces. The molecular dipole of methanol is oriented toward the cation and the COH plane of the radical is aligned along a diagonal of the square.

These results demonstrate that electron spin-echo modulation analysis provides a new and powerful approach for understanding the geometry of adsorbed radicals and molecules relative to the surface in zeolites and probably on other insulating surfaces. We expect that additional definitive geometrical information can be obtained by using selective deuteration of the adsorbed molecules and exchange of paramagnetic cations into the surfaces.

Acknowledgment. This research was supported by the U.S. Department of Energy under Contract EY-76-S-02-2086.

References and Notes

(1) J. H. Lunsford, *Catal. Rev.*, **8**, 135 (1973).
(2) L. Kevan, M. K. Bowman, P. A. Narayana, R. K. Boeckman, V. F. Yudanov, and Yu. D. Tsvetkov, *J. Chem. Phys.*, **63**, 409 (1975).
(3) P. A. Narayana, M. K. Bowman, L. Kevan, V. F. Yudanov, and Yu. D. Tsvetkov, *J. Chem. Phys.*, **63**, 3365 (1975).
(4) V. F. Yudanov, Yu. A. Grishin, and Yu. D. Tsvetkov, *J. Struct. Chem. (Engl. Transl.)*, **16**, 694 (1975).
(5) S. Schlick, P. A. Narayana, and L. Kevan, *J. Chem. Phys.*, **64**, 3153 (1976).
(6) P. A. Narayana and L. Kevan, *J. Chem. Phys.*, **65**, 3379 (1976).
(7) T. Ichikawa, L. Kevan, M. K. Bowman, S. A. Dikanov, and Yu. D. Tsvetkov, *J. Chem. Phys.*, **71**, 1167 (1979).
(8) M. Narayana and L. Kevan, *J. Chem. Phys.*, in press.
(9) T. Ichikawa and L. Kevan, *J. Chem. Phys.*, in press.
(10) P. A. Narayana, D. Becker, and L. Kevan, *J. Chem. Phys.*, **68**, 652 (1978).
(11) T. Ichikawa, L. Kevan, and P. A. Narayana, *J. Chem. Phys.*, **71**, 3792 (1979).
(12) T. Ichikawa, L. Kevan, and P. A. Narayana, *J. Phys. Chem.*, **83**, 3378 (1979).
(13) W. B. Mims and J. L. Davis, *J. Chem. Phys.*, **64**, 4836 (1979).
(14) L. Kevan in "Time Domain Electron Spin Resonance", L. Kevan and R. N. Schwartz, Ed., Wiley-Interscience, New York, 1979, Chapter 8.
(15) J. A. Rabo, Ed. "Zeolite Chemistry and Catalysis", *ACS Monogr.*, **No. 171** (1976).
(16) S. A. Dikanov, V. F. Yudanov, R. I. Samoilova, and Yu. D. Tsvetkov, *Chem. Phys. Lett.*, **52**, 520 (1977).
(17) L. Kevan, *Actions Chim. Biol. Radiat.*, **13**, 57 (1969).
(18) W. B. Mims and J. Peisach, *J. Chem. Phys.*, **69**, 4921 (1978).
(19) W. B. Mims, *Phys. Rev. B*, **5**, 2409 (1972).
(20) P. A. Narayana and L. Kevan, *J. Magn. Reson.*, **26**, 437 (1977).
(21) L. Pauling, "The Nature of the Chemical Bond", 3rd ed., Cornell University Press, Ithaca, N.Y., 1960, p 514.
(22) E. V. Ivash and D. M. Dennison, *J. Chem. Phys.*, **21**, 1804 (1953).